Back-angle anomalies in ^{6}Li scattering from ^{40}Ca and ^{44}Ca†

H. Bohn,* K. A. Eberhard,‡ R. Vandenbosch, K. G. Bernhardt,‡ R. Bangert,§ and Y-d. Chan
Nuclear Physics Laboratory, University of Washington, Seattle, Washington 98195
(Received 1 November 1976)

Angular distributions for the elastic and inelastic scattering of 30 MeV ^{6}Li ions from ^{40}Ca and ^{44}Ca have been measured. At backward angles (110°–180°) the cross sections for both elastic and inelastic scattering are an order of magnitude larger for ^{6}Li + ^{40}Ca than for ^{6}Li + ^{44}Ca. The results are compared with the anomalies observed in α and ^{3}He scattering. The difference between the back-angle scattering for ^{40}Ca and ^{44}Ca is discussed in terms of the relative number of competing direct reaction channels capable of carrying away large amounts of angular momentum.

[NUCLEAR REACTIONS ^{40,44}Ca(^{6}Li,^{6}Li), (^{6}Li,^{6}Li'), E=30 MeV; measured $\sigma(E,\theta)$; calculated $\sigma(E,\theta)$, optical model, coupled-channel, Hauser-Feshbach calculations.]

I. INTRODUCTION

The back-angle anomalies for elastic and inelastic scattering of α particles from the Ca isotopes and some lighter nuclei are well established: Order-of-magnitude differences in back-angle cross sections are observed for neighboring target nuclei.[1] In order to see if similar effects also show up for projectiles more complex than α particles we have investigated the scattering of ^{6}Li ions from ^{40}Ca and ^{44}Ca at appropriate energies. Previous experimental work with projectiles other than α particles has concentrated on ^{3}He scattering where similar anomalies have been observed although less pronounced than for α particles.[2-6] The only relevant experimental heavy-ion study, the scattering of ^{16}O from ^{40}Ca and ^{48}Ca by the Argonne group,[7] shows no indication of anomalous cross sections for either ^{40}Ca or ^{48}Ca at the relatively low energies studied.

Most of the existing data of Li scattering in the Ca region are confined to the forward-angle hemisphere.[8-11] Back-angle data are only available from the work of Davydov *et al.*[9] These authors used a natural Ca target and thus could not study possible differences between ^{40}Ca and ^{44}Ca. In this paper we report angular distributions for ^{6}Li + ^{40}Ca and ^{6}Li + ^{44}Ca elastic and inelastic scattering. Particular emphasis is given to the back-angle hemisphere to study possible differences in ^{6}Li + ^{40}Ca and ^{6}Li + ^{44}Ca scattering. A bombarding energy of 30 MeV (lab) was chosen to be in the same energy range above the Coulomb barrier where the strongest backward anomalies have been observed in α scattering.

In Sec. II the experimental procedure is described. The experimental results are presented in Sec. III and optical model (OM), coupled-channel (CC), and statistical model calculations are described in Sec. IV.

II. EXPERIMENTAL PROCEDURE

A ^{6}Li beam from the University of Washington FN tandem accelerator was focused onto CaF_2 targets on 20 μg/cm^2 carbon backings in the center of the 150 cm scattering chamber. The thickness of the $^{40}CaF_2$ target was 470 μg/cm^2 (^{40}Ca: 241 μg/cm^2); that of $^{44}CaF_2$ was 570 μg/cm^2 (^{44}Ca: 306 μg/cm^2) thick. The enrichment of the ^{40}Ca target was 99.965% and of the ^{44}Ca target, 98.55%. The energy losses of 30 MeV Li ions in the CaF_2 targets are 250 and 290 keV, respectively. A standard dE/dx E technique was used to detect ^{6}Li and α-particle events in three solid state counter telescopes. During the measurements a monitor detector was placed at θ_{lab} = 35° so that cross section determinations could be made independent of possible target inhomogeneities. A resolution of typically 200 to 500 keV, depending on the angular range, was obtained, and was mainly caused by the thickness of the target. Beam currents ranged between 50 and 100 nA and were mainly restricted by the Li-source conditions. The absolute error of the experimental cross sections is ±10%. The statistical errors are indicated in the figures.

III. EXPERIMENTAL RESULTS

Angular distributions for the elastic scattering of ^{6}Li from ^{40}Ca and ^{44}Ca at a bombarding energy of 30 MeV (lab) are shown in Fig. 1. The cross sections from these isotopes are almost identical at angles smaller than 90°. At angles of 120° and larger, a difference of more than one order of magnitude is observed. At these angles the ^{6}Li + ^{40}Ca data oscillate with the overall cross section

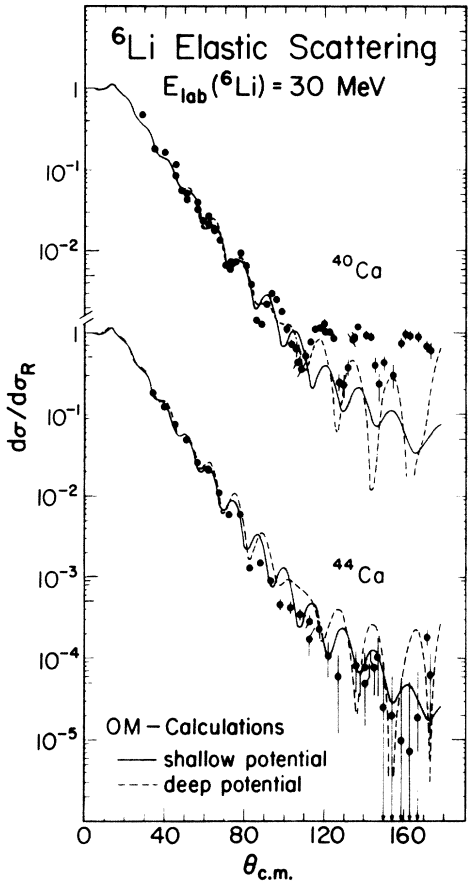

FIG. 1. Angular distributions for ^{6}Li elastic scattering from ^{40}Ca and ^{44}Ca. The lines represent two different sets of optical model potentials (see Table I).

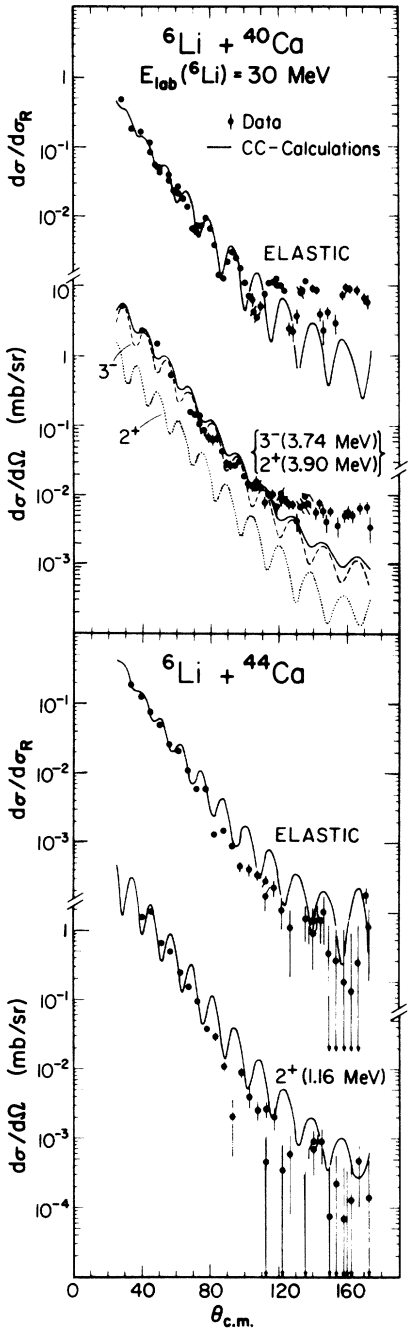

FIG. 2. Angular distributions of ^{6}Li elastic and inelastic scattering from ^{40}Ca and ^{44}Ca shown together with the results of coupled-channels calculations (see Table I and text).

essentially remaining constant. In contrast, the ^{6}Li + ^{44}Ca angular distribution falls off rapidly and continuously with angle and only rises again at the most backward angles ($\theta \approx 170°$). Even at this angle the cross section is still about five times smaller than for ^{6}Li + ^{40}Ca. The poor counting statistics for ^{6}Li + ^{44}Ca at backward angles, due to the small cross sections (<1 μb/sr; about 2 to 3 counts within 8 h), do not allow a rigorous statement on possible back-angle oscillations, although it seems to be indicative from Fig. 1 that no regular oscillations as seen for ^{6}Li + ^{40}Ca are present in ^{6}Li + ^{44}Ca.

It is interesting to note that Fink, Strohbusch, and Zeidman[10] have measured elastic-scattering angular distributions for ^{6}Li on ^{40}Ca, ^{44}Ca, ^{48}Ca, and ^{50}Ti between 10 and 100° at an incident energy of 32 MeV. The slopes of these angular distributions are similar in all cases, but the diffraction structure observed is considerably enhanced for ^{6}Li on ^{40}Ca.

The inelastic scattering results are presented in Fig. 2. Due to the expected small cross sections at backward angles, relatively thick targets were used and cross sections could only be obtained for the inelastic scattering to the 3.74 MeV (3^-) state [with possible contributions from the 3.90 MeV (2^+) state] in ^{40}Ca and for the 1.16 MeV (2^+) state in ^{44}Ca. Comparing the inelastic cross

sections for ^{6}Li+^{40}Ca and ^{6}Li+^{44}Ca, qualitatively the same behavior is found as for the elastic scattering: Although the states are different in spin and excitation energy the cross sections for both isotopes are remarkably similar at angles smaller than about 80°, i.e., they do not differ by more than a factor of 2. At backward angles, however, the cross section for ^{40}Ca is one to two orders of magnitude larger than for ^{44}Ca. For both isotopes the inelastic cross sections at backward angles are of the same order of magnitude as for elastic scattering at these angles.

IV. ANALYSIS

A. Optical model calculations

In our optical model analysis we have started with potentials obtained previously in fits to forward-angle data. These potentials also gave a reasonable fit to the back-angle data for ^{44}Ca but not for ^{40}Ca. We have therefore made slight adjustments to these potentials so as to improve the fit to our ^{44}Ca data at all angles and ^{40}Ca data at angles forward of 110°. The real and imaginary potentials were constrained to have the same geometry and all parameters were also constrained to be the same for the two isotopes. The results obtained with both "shallow" ($V\sim 25$ MeV) and "deep" ($V\sim 250$ MeV) Woods-Saxon potentials are shown with the data in Fig. 1. These potentials were derived from those of Davydov *et al.*[9] (shallow potential) and of Strohbusch[12] (deep potential). The parameter values used are listed in Table I.

As can be seen from Fig. 1 the calculated angular distributions with the shallow and the deep potentials are equivalent at forward angles. In comparing the OM cross sections with the data it is seen that for ^{6}Li+^{44}Ca the overall behavior is correctly reproduced over the entire angular range whereas for ^{6}Li+^{40}Ca the data are reproduced at forward angles ($<\sim 100°$) only. At angles of 120° and larger the experimental cross sections are up to one order of magnitude larger than predicted. This resembles similar results in ^{3}He and α-particle scattering (cf. Sec. V).

TABLE I. Parameters used in the optical model and coupled-channel calculations. The coupling scheme is 0^+(g.s.)-2^+-3^- in the coupled-channel calculations.

	V (MeV)	r_0[a] (fm)	a_0 (fm)	W (MeV)	r_c (fm)	β_2	β_3
			^{40}Ca				
OM	25.7	1.83	0.65	18.0	1.83	...	...
	250.0	1.41	0.65	35.0	1.41	...	...
CC	25.7	1.83	0.65	12.6	1.83	0.09	0.19
			^{44}Ca				
OM	25.7	1.83	0.65	18.0	1.83	...	...
	250.0	1.41	0.65	35.0	1.41	...	...
CC	25.7	1.83	0.65	12.6	1.83	0.19	0.15

[a] $R = r_0 A_T^{1/3}$.

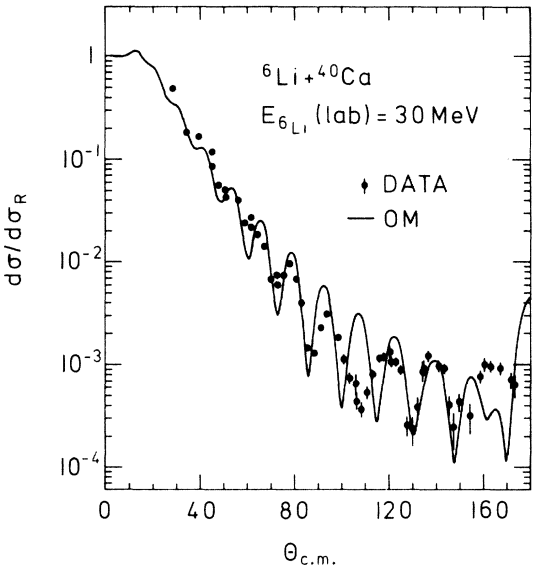

FIG. 3. Fit to the ^{40}Ca+^{6}Li elastic scattering with an l-dependent potential using the parameters for the shallow potential (see Table I) with $l_c = 16$ and $\Delta l = 4.0$.

It has previously been shown that an improved optical model fit to back-angle α-particle scattering can be achieved using an l-dependent potential. We therefore tried to fit the scattering for ^{6}Li+^{40}Ca starting with the shallow potential (see Table I) and introducing an explicit l dependence with the imaginary part of the potential multiplied by a form factor $\{1+\exp[(l-l_c)/\Delta l]\}^{-1}$. The best fit is shown in Fig. 3 and was obtained using $l_c = 16$ and $\Delta l = 4.0$ and by averaging over the experimental angular resolution of $\Delta\theta = 1.5°$. Compared with the fit as obtained with the conventional four-parameter shallow potential (see Fig. 1) the l dependence introduces more structure. The data are not reproduced in detail but the overall agreement is improved. Especially in the backward-angle region the fit gives the right order of magnitude.

B. Coupled-channel calculations

The fact that the inelastic cross sections are comparable to those for elastic scattering has led us to analyze the data in terms of coupled-channel calculations. The curves shown in Fig. 2 were calculated with the computer code JUPITOR by Tamura.[13] Vibrational coupling and a real form factor were used. A coupling scheme 0^+ (g.s.)-2^+-3^- was adopted for both ^{6}Li+^{40}Ca and ^{6}Li+^{44}Ca

inelastic scattering. This allows a consistent calculation of the scattering to the 3^- (3.74 MeV) state in ^{40}Ca and the 2^+ (1.16 MeV) state in ^{44}Ca, which were the only states for which experimental data were obtained. The calculated cross section for the 3^- (3.31 MeV) state in ^{44}Ca was in agreement with the cross section observed at the few angles where it could be resolved. The coupling parameters β were taken from the α-scattering work of Trombik, Eberhard, and Eck[14]; they were corrected for the different radii R used in Ref. 14 and our analysis, since βR is the relevant quantity rather than β itself. All parameters used in the coupled-channel calculations of Fig. 2 are summarized in Table I. The imaginary part of the potential was reduced by 30% to take into account the reduction in absorption due to the explicit coupling of the above excited states.

Since the coupled-channel calculations are lengthy and costly, we have used only one of the two equivalent optical model potentials (see Table I). Inspection of Fig. 2 shows that the coupled-channel (CC) cross sections for ^{6}Li + ^{40}Ca and ^{6}Li + ^{44}Ca elastic scattering are essentially equal to those obtained with the optical model as shown in Fig. 1. Slight differences are observed only at backward angles. In particular we would like to point out that the order-of-magnitude deviation between experimental and calculated elastic-scattering cross sections for ^{6}Li + ^{40}Ca is not remedied by coupling the 2^+ (3.90 MeV) and 3^- (3.74 MeV) states, the strongest inelastic channels observed, to the elastic channel. The inelastic scattering ^{6}Li + ^{40}Ca to the 2^+ (3.90 MeV) and the 3^- (3.74 MeV) states could not be resolved in the experiment. Therefore CC calculations for both states are shown in Fig. 2, and the sum (solid line) is compared with the data. The calculations indicate that the major contribution to the unresolved doublet arises from scattering to the strongly collective 3^- state. The magnitude and the slope of the data at forward angles are correctly accounted for in the calculations, although at some angles the phase is not correctly reproduced. A better reproduction of the phase could be expected by a slight adjustment of the potential, i.e., by a parameter search in the CC calculations which was not undertaken here. A more detailed description of the data is likely to be obtained by using different parameters for ^{40}Ca and ^{44}Ca and/or by using different form factors for the real and imaginary part of the potential. Such refinements are not expected to change the order-of-magnitude discrepancy between the calculated and measured back-angle inelastic cross sections.

Experimental and calculated cross sections for elastic and inelastic ^{6}Li + ^{44}Ca scattering are compared in the lower part of Fig. 2. At backward angles the calculated cross sections, in contrast to ^{6}Li + ^{40}Ca, are slightly larger than the experimental ones which clearly demonstrates the order-of-magnitude difference between the experimental cross sections at backward angles for the scattering of ^{6}Li on ^{40}Ca and ^{44}Ca.

C. Statistical model calculations

In this section we estimate possible compound-nuclear contributions in the data of Figs. 1 and 2. Since compound cross sections are symmetric about 90°, an increase of the cross section toward backward angles such as seen for ^{6}Li + ^{40}Ca scattering could be indicative of a certain compound contribution. Therefore detailed Hauser-Feshbach (HF) calculations have been performed using Stokstad's procedure and computer code STAT2.[15]

In the compound-nuclear picture ^{6}Li + ^{40}Ca scattering at 30 MeV forms the compound nucleus ^{46}V at an excitation energy of about 42 MeV. Among the many open decay channels of this highly excited compound nucleus the most important ones are the n+ ^{45}V, p+ ^{45}Ti, d+ ^{44}Ti, ^{3}He+ ^{43}Sc, α + ^{42}Sc, and ^{6}Li + ^{40}Ca. The evaluation of the decay probabilities into these channels and, thus, the computation of the denominator in the Hauser-Feshbach formula requires knowledge of the energies, spins, and parities of all the final states in the residual nuclei. For low-lying states, where these quantities are known, the decay probability was calculated individually. Above this energy, referred to as E_{cut} and listed in Table II, a level density formula has been employed for higher excitation energies. To be as realistic as possible in the calculations, individual parameters for the optical model potentials and for the level densities were used and were taken from the literature. All the quantities entering the calculations are listed in Table II.

The calculated cross sections are orders of magnitude smaller than the experimental ones. At 0° and 180° the calculated HF cross section is largest and is 2.5×10^{-5} mb/sr for ^{6}Li + ^{40}Ca elastic scattering; at 90° the cross section is 10^{-6} mb/sr. The corresponding experimental cross section near 180° is about 5×10^{-3} mb/sr and about 10^{-1} mb/sr at 90°. Also for ^{6}Li + ^{44}Ca scattering (cf., Figs. 1 and 2) calculated compound-nuclear cross sections are obtained which are orders of magnitude smaller than the experimental cross sections. Even taking into account the possibility that the absolute magnitude of the calculated compound-nuclear cross sections can be wrong by about a factor of 5 there still remains a discrepancy of more than an order of magnitude between the calculations and the experiment. It can therefore be

TABLE II. Statistical model and optical model parameters used in the Hauser-Feshbach calculations. The level density notation is that of Ref. 22. The various decay modes of the compound nucleus are labeled by the particle by which the compound nucleus decays.

	Decay channels					
	^{6}Li + ^{40,44}Ca	α + ^{42,46}Sc	^{3}He + ^{43,47}Sc	d + ^{44,48}Ti	p + ^{45,49}Ti	n + ^{45,49}V
a/A [a] (MeV^{-1})	0.148, 0.162	0.146, 0.151	0.170, 0.145	0.162, 0.143	0.167, 0.151	0.171, 0.150
Δ [b] (MeV)	3.87, 3.27	0	1.64, 1.54	3.37, 3.27	1.73, 1.73	1.64, 1.64
E_{cut} [c] (MeV)	6.91, 3.77	1.59, 0.991	2.09, 1.39	3.37, 4.05	4.81, 2.66	0, 1.14
V (MeV)	25.7	103.6	177.4	$61.3 - 0.45E_{c.m.}$	$\left.\begin{matrix}57\\58.58\end{matrix}\right\} - 0.31E_{c.m.}$	$\left.\begin{matrix}56.8\\54.8\end{matrix}\right\} - 0.31E_{c.m.}$
r_0 [d] (fm)	1.2	1.52	1.14	1.15	1.17	1.17
a_0 (fm)	0.693	0.54	0.68	0.87	0.75	0.75
W [e] (MeV)	22	17.5	19.9	14	$\left.\begin{matrix}12.07\\13.02\end{matrix}\right\} - 0.24E_{c.m.}$	$\left.\begin{matrix}13.27\\12.27\end{matrix}\right\} - 0.24E_{c.m.}$
r_i [d] (fm)	1.2	1.52	1.64	1.37	1.32	1.26
a_i (fm)	0.693	0.54	0.79	0.70	0.53, 0.61	0.58
r_c [d]	0.914	1.52	1.40	1.15	1.38	1.38
Ref. for optical model	f	g	h	i	j	j

[a] U. Facchini and E. Saetta-Menichella, Energ. Nucl. (Milan) 15, 54 (1968).
[b] A. Gilbert and A. G. W. Cameron, Can. J. Phys. 43, 1446 (1965).
[c] E_{cut}: energy above which discrete levels were "unknown" and continuum level densities were used.
[d] $R = r_0(A_1^{1/3} + A_2^{1/3})$ for ^{6}Li, $R = r_0 A^{1/3}$ otherwise.
[e] Surface-type for d, p, n; volume-type otherwise.
[f] Reference 9.
[g] J. R. Priest and J. S. Vincent, Phys. Rev. 182, 1121 (1969).
[h] R. W. Barnard and G. D. Jones, Nucl. Phys. A111, 17 (1968).
[i] C. M. Perey and F. G. Perey, Phys. Rev. 132, 755 (1963).
[j] F. D. Becchetti, Jr., and G. W. Greenlees, Phys. Rev. 182, 1190 (1969).

concluded that compound-nuclear processes are negligible for the reactions which are of interest here and that the observed anomaly in the back-angle cross section is not due to compound elastic scattering; it arises primarily from a direct reaction process. The same conclusion has recently been obtained for elastic α scattering.[16]

In Table III total compound cross sections, integrated over angle and the entire range of excitation energy in the residual nuclei, are given for various decay channels to show the main mode of decay of the compound nucleus. Comparing the results for ^{40}Ca and ^{44}Ca one observes that the total cross sections for the ^{6}Li as well as for the α channels are essentially equal. The main mode of decay for ^{46}V is the proton channel; for ^{50}V the neutron channel is strongest. This difference is owing to different Q values. It is clearly seen that only a negligible fraction of the compound nucleus decays into those channels which are studied in this paper.

TABLE III. Calculated total compound-nuclear cross sections for ^{6}Li-induced reactions on ^{40}Ca and ^{44}Ca. The various reaction channels are labeled by the particle through which the compound nucleus decays. The parameters used in the Hauser-Feshbach calculations are listed in Table II. The cross sections are summed over the respective range of excitation energies in the corresponding residual nuclei.

	σ (mb)						
Target	n	p	d	^{3}He	α	^{6}Li	$\sum$(all channels)
^{40}Ca	308	1189	23	2.2	51	0.07	1573
^{44}Ca	1232	334	12	0.26	68	0.03	1646

V. DISCUSSION

A. Comparison with ^{3}He and α scattering

Back-angle anomalies are well known in elastic α scattering and have been observed for target nuclei such as ^{40}Ca, ^{41}Ca, ^{39}K, ^{40}K, ^{36}Ar, and ^{38}Ar. Recently back-angle integrated cross sections for elastic scattering of ^{3}He and α particles between 140 and 180° as a function of target mass have been derived from existing experimental data by Eberhard *et al.*[2] It is demonstrated by these authors, in agreement with the earlier work of Oeschler *et al.*,[17] that the enhancement of the back-angle

TABLE IV. Comparison of angle-integrated cross sections for ^{3}He, α, and ^{6}Li projectiles. The integrated cross sections $\sigma_{int} = \int_{140°}^{180°} d\sigma$ were obtained at bombarding energies 23–27 MeV for α particles, 28–29 MeV for ^{3}He, and 30 MeV for ^{6}Li.

Projectile	σ_{int} (μb) ^{40}Ca	^{44}Ca	Ratio ^{40}Ca/^{44}Ca
^{3}He	40	8	5
α	2000	80	25
^{6}Li	7	0.5	14

cross section disappears whenever at least one pair of $f_{7/2}$ neutrons are added to the closed shell core of ^{40}Ca. The addition of only one $f_{7/2}$ neutron has but little effect on the backward enhancement: The back-angle cross sections for ^{41}Ca and ^{40}K are almost as large as those for ^{40}Ca. This systematic also holds for ^{3}He scattering, although the experimental data are not as complete at present as for α scattering.[2]

For ^{6}Li scattering the only data available for comparison between ^{40}Ca and ^{44}Ca are presented in this paper. Obviously the experimental results are in agreement with the above systematics. In Table IV we have integrated back-angle cross sections between 140 and 180° for the elastic scattering of ^{3}He, α, and ^{6}Li projectiles from ^{40}Ca and ^{44}Ca. The values for ^{3}He and α projectiles were taken from Ref. 2 and correspond to bombarding energies of 23 to 27 MeV for α particles and of 28 through 29 MeV for ^{3}He scattering. The ^{6}Li integrated cross section was calculated from the data in Fig. 1. For the target nucleus ^{40}Ca the back-angle cross section for α scattering is about 50 times larger than for ^{3}He scattering and about 300 times larger than for ^{6}Li scattering. For ^{44}Ca these ratios are not quite as large, although the α scattering cross sections are also significantly larger. The absolute magnitude of the back-angle cross sections correlate with the stability of the projectile, and may simply reflect the fact that it is easier for ^{6}Li and ^{3}He to be broken up so that the probability of survival for back-angle scattering is reduced. In column 4 of Table IV the ratios for the scattering of these projectiles from ^{40}Ca and ^{44}Ca are listed. Strongest enhancement is observed for α particles again. It is interesting to note that the ^{40}Ca/^{44}Ca cross section ratio for ^{6}Li scattering is larger than for ^{3}He scattering, although the absolute back-angle cross sections are much smaller. Since both the ^{3}He and the ^{6}Li data were taken at only one energy this result has to be taken with some caution. On the other hand no strong energy dependence of the α back-angle scattering ratio has been observed.

B. Role of competing direct reaction channels

In Sec. IV A on the optical model analysis of our data it was shown that the description of the back-angle anomaly for ^{40}Ca + ^{6}Li scattering could be improved by using an l-dependent potential, suggesting that the differences observed for the two isotopes could be ascribed to a slightly reduced probability for absorption for the highest partial waves for ^{40}Ca compared with ^{44}Ca. Such a difference might arise if the number or angular momentum matching conditions for the competing direct reaction channels are different. Such considerations have been successful in explaining the dramatic differences between the elastic scattering in the ^{16}O+ ^{16}O and ^{18}O+ ^{18}O systems.[18] Some indirect evidence that such an effect might be occurring here is provided by a recent comparative study of the direct reaction channels for ^{16}O-induced reactions with ^{40}Ca and ^{44}Ca.[19] It was found that the sum of the measured cross sections for inelastic scattering and for transfer reactions in which 1 to 5 nucleons are transferred is about 150 mb for ^{44}Ca and only about 80 mb for ^{40}Ca. No corresponding data for ^{6}Li or α-induced reactions are available, but since the inelastic scattering would lead to the same levels in the target nuclei and since most of the transfer was observed to correspond to transfer from the projectile to the target, a similar behavior for these systems might be expected.

To explore the idea that the difference in absorption might arise from differences in the number or angular momentum matching conditions of the direct reaction channels for the two isotopes, we have constructed histograms which show the number of states versus exit channel angular momentum for each kind of channel and for each of the two target nuclei. These histograms, shown in Fig. 4, are similar to ones presented by Eberhard,[20] although we have only included direct channels expected to have large cross sections in the present comparison. The maximum exit channel angular momentum has been constructed from the sum of the spin of the particular level of the heavy reaction product and the maximum orbital angular momentum (that for which $T_l = \frac{1}{2}$ in an optical model calculation) for the appropriate exit channel kinetic energy. We have neglected the spin of the light particle and the change in the optical potential due to the change in mass of the light particle following nuclear pickup as these effects will not affect the *relative* behavior of the curves for the two isotopes. In a few instances the spins of the low-lying levels considered are not known and have been assumed to be 2. These contributions are shown by dashed lines.

It can be seen in Fig. 4 that there are more chan-

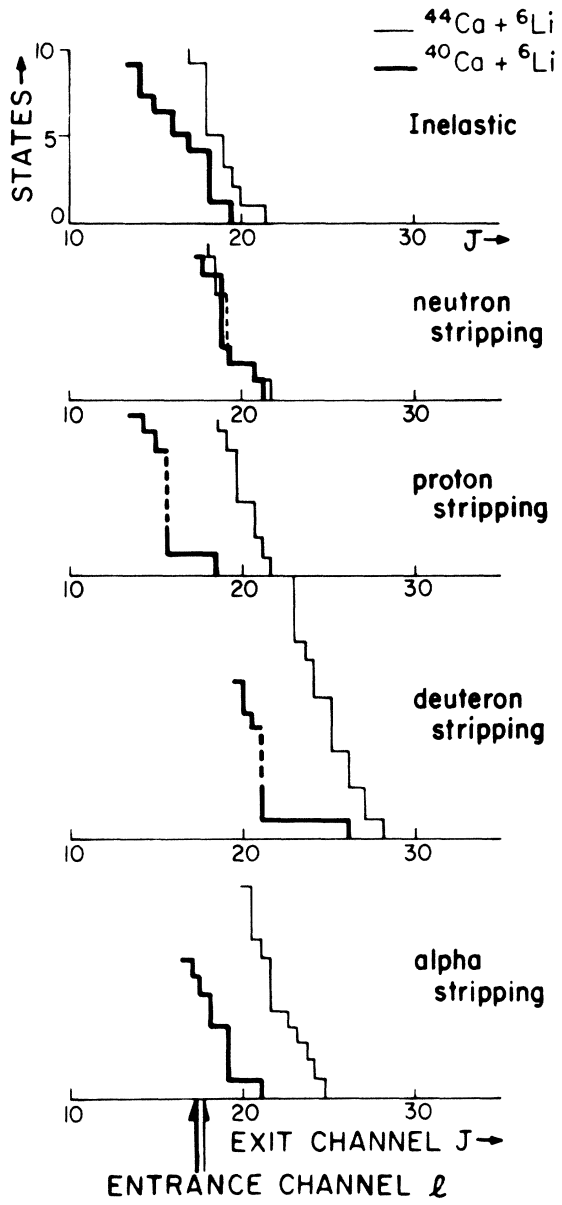

FIG. 4. The number of states for various types of reaction channels are plotted as a function of the exit channel angular momentum. The arrows at the bottom of the figure indicate l values for which $T_l = \frac{1}{2}$ in the entrance channel. The heavy curves are for ^{6}Li+^{40}Ca and the lighter curves are for ^{6}Li+^{44}Ca.

nels capable of carrying away larger amounts of angular momentum for ^{44}Ca than for ^{40}Ca for each kind of reaction channel except for 1-neutron transfer where the numbers are comparable. The differences between the two isotopes correlate with Q values, with additional contributions arising from differences in level densities for the final nuclei. We have not considered reactions where particles are picked up by the projectile, as the Q values are much less favorable and the Argonne study[19] shows that the cross sections for such pickup are smaller, at least for ^{16}O-induced reactions. The comparison of Fig. 4 supports the suggestion that the competition of the direct reaction channels with the elastic channel may be stronger for ^{44}Ca than for ^{40}Ca. Since the *differences* between the Q values for the two isotopes for inelastic and transfer reactions leading to the same respective final nuclei will be independent of the projectile, a similar effect is to be expected for other projectiles, provided that other quantities such as level densities, etc. remain similar.

VI. SUMMARY

Cross sections for the elastic and inelastic scattering of ^{6}Li ions from ^{40}Ca and ^{44}Ca have been measured. The cross sections are almost identical at forward angles; at angles of 120° or larger, however, they differ by more than one order of magnitude. It is shown that it is not possible to reproduce the elastic-scattering angular distribution at backward angles for *both* nuclei with the same optical model parameters. Using the same procedure as for α-particle scattering an l-dependent absorption in the potential was tried and led to an improved description of the ^{6}Li+^{40}Ca scattering at backward angles. In terms of the l-dependent absorption model[18,20,21] this indicates that the number of available direct reaction channels which can carry the highest angular momenta from the elastic channel, i.e., $l \approx k \times R$, is considerably smaller for ^{6}Li+^{40}Ca than for ^{6}Li+^{44}Ca. This idea is supported by an examination of the number of direct reaction channels capable of carrying away large amounts of angular momentum.

Hauser-Feshbach calculations showed that compound-nuclear contributions are orders of magnitude smaller than the measured cross sections and thus are negligible here (see Sec. IV C).

The back-angle integrated cross section for elastic scattering of ^{6}Li ions is about 15 times larger for ^{40}Ca than for ^{44}Ca. It is, however, more than two orders of magnitude smaller than comparable α scattering cross sections, and about one order of magnitude smaller than those for ^{3}He. A possible reason could be the small binding energy of only 1.47 MeV for $^6\text{Li} \rightarrow \alpha + d$ which makes a breakup at small impact parameters (which correspond to backward scattering) likely.

Inelastic ^{6}Li scattering to the 3.74 MeV (3^-) state in ^{40}Ca and to the 1.16 MeV (2^+) state in ^{44}Ca shows qualitatively the same behavior at backward angles as the elastic scattering.

The investigation of the back-angle anomaly with additional projectiles such as ^{12}C and ^{16}O at higher energies would be interesting. Furthermore, a more systematic study of ^{6}Li scattering from target nuclei such as $^{41,42}Ca$, ^{48}Ca, the K isotopes, and the Ar isotopes is needed to answer the question whether the $f_{7/2}$-neutron systematic observed for α scattering also holds for ^{6}Li scattering.

We would like to thank G. Rohrbaugh, C. Linder, and the tandem operators for producing and maintaining the ^{6}Li beam during the experiment.

---

†Work supported in part by USERDA; research work of K. A. Eberhard supported in part by NATO research grant No. 1193.

*Permanent address: Physik-Department E12, Technische Universität München, D-8046 Garching, Germany.

‡ Permanent address: Sektion Physik der Universität München, D-8046 Garching, Germany.

§Permanent address: Institut für Kernphysik, Universität zu Köln, D-5000 Köln, Germany.

[1]For a recent survey see J. S. Eck, W. J. Thompson, K. A. Eberhard, J. Schiele, and W. Trombik, Nucl. Phys. A255, 157 (1975), and literature cited therein.

[2]For a recent survey see, e.g., K. A. Eberhard, M. Wit, J. Schiele, W. Trombik, W. Zipper, and J. P. Schiffer, Phys. Rev. C 14, 2332 (1976).

[3]J. W. Luetzelschwab and J. C. Hafele, Phys. Rev. 180, 1023 (1969).

[4]H. Breuer and H. P. Morsch, Nucl. Phys. A255, 449 (1975).

[5]H. P. Morsch and H. Breuer, Nucl. Phys. A208, 255 (1973).

[6]H. P. Morsch and R. Santo, Nucl. Phys. A179, 401 (1972).

[7]K. O. Groeneveld, L. Meyer-Schützmeister, A. Richter, and U. Strohbusch, Phys. Rev. C 6, 805 (1972).

[8]K. Bethge, C. M. Fou, and R. W. Zurmühle, Nucl. Phys. A123, 521 (1969).

[9]V. V. Davydov, B. G. Novatskii, A. A. Ogloblin, S. B. Sakuta, D. N. Stepanov, and V. I. Chuev, Izv. Akad. Nauk. SSSR, Ser. Phys. 35, 2399 (1971) [Bull. Acad. Sci. USSR, Phys. Ser. 35, 2176 (1971)]; V. I. Chuev, V. V. Davydov, B. G. Novatskii, A. A. Ogloblin, S. B. Sakuta, and D. N. Stepanov, J. Phys. (Paris) C 6, 157 (1971).

[10]C. L. Fink, U. Strohbusch, and B. Zeidman, Argonne National Laboratory Progress Report, 1973 (unpublished), p. 73.

[11]L. T. Chua, F. D. Becchetti, J. Jänecke, and F. Milder, Bull. Am. Phys. Soc. 20, 716 (1975); and Nucl. Phys. A273, 243 (1976).

[12]U. Strohbusch, in Proceedings of the International Symposium on Cluster Structure of Nuclei and Transfer Reactions Induced by Heavy Ions, INS, ICPR, Tokyo, March 1975 (unpublished), p. 506.

[13]T. Tamura, Rev. Mod. Phys. 37, 679 (1965); Oak Ridge National Laboratory Report No. 4152, 1967 (unpublished).

[14]W. Trombik, K. A. Eberhard, and J. S. Eck, Phys. Rev. C 11, 685 (1975).

[15]R. G. Stokstad, STAT2 —A Hauser-Feshbach Computer Code, Oak Ridge National Laboratory, 1975 (unpublished).

[16]K. A. Eberhard, T. H. Braid, T. Renner, J. P. Schiffer, and S. Vigdor, Phys. Rev. C 14, 548 (1976).

[17]H. Oeschler, H. Schrötter, H. Fuchs, L. Baum, G. Gaul, H. Lüdecke, R. Santo, and R. Stock, Phys. Rev. Lett. 28, 694 (1972).

[18]R. W. Shaw, R. Vandenbosch, and M. K. Mehta, Phys. Rev. Lett. 25, 457 (1970).

[19]S. E. Vigdor, in Symposium on Macroscopic Features of Heavy-Ion Collisions, Argonne National Laboratory, 1–3 April, 1976 (unpublished).

[20]K. A. Eberhard, Phys. Lett. 33B, 343 (1970).

[21]R. A. Chatwin, J. S. Eck, D. Robson, and A. Richter, Phys. Rev. C 1, 795 (1970).

[22]D. L. Hanson, R. G. Stokstad, K. A. Erb, C. Olmer, and D. A. Bromley, Phys. Rev. C 9, 929 (1974).